The EMBO Journal (2008) 27, 2681–2690 | © 2008 European Molecular Biology Organization | All Rights Reserved 0261-4189/08
www.embojournal.org

THE EMBO JOURNAL

G9a/GLP complexes independently mediate H3K9 and DNA methylation to silence transcription

Makoto Tachibana[1,2,*], Yasuko Matsumura[1], Mikiko Fukuda[1], Hiroshi Kimura[3] and Yoichi Shinkai[1,2,*]

[1]Experimental Research Center for Infectious Diseases, Institute for Virus Research, Kyoto University, Sakyo-ku, Kyoto, Japan, [2]Graduate School of Biostudies, Kyoto University, Sakyo-ku, Kyoto, Japan and [3]Graduate School of Frontier Biosciences, Osaka University, Suita, Osaka, Japan

Methylation of DNA and lysine 9 of histone H3 (H3K9) are well-conserved epigenetic marks for transcriptional silencing. Although H3K9 methylation directs DNA methylation in filamentous fungi and plants, this pathway has not been corroborated in mammals. G9a and GLP/Eu-HMTase1 are two-related mammalian lysine methyltransferases and a G9a/GLP heteromeric complex regulates H3K9 methylation of euchromatin. To elucidate the function of G9a/GLP-mediated H3K9 methylation in the regulation of DNA methylation and transcriptional silencing, we characterized ES cells expressing catalytically inactive mutants of G9a and/or GLP. Interestingly, in ES cells expressing a G9a-mutant/GLP complex that does not rescue global H3K9 methylation, G9a/GLP-target genes remain silent. The CpG sites of the promoter regions of these genes were hypermethylated in such mutant ES cells, but hypomethylated in *G9a*- or *GLP*-KO ES cells. Treatment with a DNA methyltransferase inhibitor reactivates these G9a/GLP-target genes in ES cells expressing catalytically inactive G9a/GLP proteins, but not the wild-type proteins. This is the first clear evidence that G9a/GLP suppresses transcription by independently inducing both H3K9 and DNA methylation.

The EMBO Journal (2008) **27,** 2681–2690. doi:10.1038/emboj.2008.192; Published online 25 September 2008
Subject Categories: chromatin & transcription
Keywords: DNA methylation; G9a; GLP; histone lysine methylation

Introduction

Genetic information of eukaryotes is stored as chromatin, which consists of genomic DNA, histones and a wide array of chromosomal proteins. Chromatin templates are subjected to various post-translational modifications to regulate many distinct biological functions (Strahl and Allis, 2000; Margueron *et al*, 2005). Among them, methylation of lysine 9 of histone H3 (H3K9) is a well-conserved epigenetic mark for heterochromatin formation and transcriptional silencing (Jenuwein, 2006). Methylation of H3K9 creates a binding site for the heterochromatin protein 1 (HP1) family molecules (Bannister *et al*, 2001; Lachner *et al*, 2001). Although recruitment of HP1 may be involved in heterochromatin formation, it is not well known how H3K9 methylation directs transcriptional silencing.

Methylation of genomic DNA is another crucial epigenetic mark for transcriptionally silent chromatin (Bird, 2002). Methylation of CpG sites regulates transcription through recruitment of the methyl CpG binding molecules or suppressing DNA binding of various transcriptional regulators such as CTCF (Wade, 2001). Furthermore, the hemimethylated CpG binding molecule(s) is important for the maintenance of DNA methylation though replication (Bostick *et al*, 2007; Sharif *et al*, 2007).

It is known that H3K9 methylation directs DNA methylation in filamentous fungi (Tamaru and Selker, 2001) and plants (Jackson *et al*, 2002). In *Neurospora crassa*, H3K9 methylation catalysed by HMTase DIM-5 directs all cytosine methylation. Similarly, in *Arabidopsis thaliana*, HMTase KRY/SUV4 catalyses H3K9 methylation and this epigenetic mark directs CMT3-mediated non-CpG methylation. However, the interplay between these epigentic marks in mammals is not well understood.

G9a and GLP/Eu-HMTase1 are two related mammalian lysine methyltransferases, both of which are crucial for H3K9 methylation (mainly mono- and di-methylation, me1 and 2) of euchromatin (Tachibana *et al*, 2002, 2005). Although G9a and GLP can form a homo- or heteromeric complex through their SET-domain interaction if they are transiently expressed, endogenous G9a and GLP mostly exist as G9a/GLP heteromer (Tachibana *et al*, 2005). Genetic analyses revealed that both G9a and GLP are essential for global H3K9me1 and 2 ((Tachibana *et al*, 2005) and Supplementary Figure S1). These findings indicate that the G9a/GLP heteromeric complex is the only functional form for global H3K9 methylation *in vivo*, even though recombinant G9a or GLP can independently methylate H3K9 *in vitro* (Tachibana *et al*, 2001, 2005).

RNA expression microarray analyses revealed that an overlapping set of genes are aberrantly expressed in *G9a*- and *GLP*-KO ES cells, indicating that G9a/GLP-mediated H3K9 methylation is involved in transcriptional silencing. Indeed, H3K9 methylation on the promoter region of one such G9a/GLP-target gene, *Mage-a2,* is significantly diminished in *G9a*- and *GLP*-KO ES cells (Tachibana *et al*, 2002, 2005). Furthermore, some studies suggest a functional interaction between G9a-mediated H3K9 methylation and DNA methylation (Xin *et al*, 2003; Estève *et al*, 2006; Feldman *et al*, 2006; Ikegami *et al*, 2007). We have also found that methylation of CpG sites of the *Mage-a2* promoter region are regulated by G9a. These sites are hypomethylated in *G9a*- and *GLP*-KO ES cells, but hypermethylated in wild-type and transgene-complemented *G9a*- or *GLP*-KO ES cells (Figure 3B).

*Corresponding authors. M Tachibana or Y Shinkai, Experimental Research Center for Infectious Diseases, Institute for Virus Research, Kyoto University, Sakyo-ku, Kyoto 606-8507, Japan.
Tel.: +81 75 751 3991; Fax: +81 75 751 3991;
E-mails: mtachiba@virus.kyoto-u.ac.jp or yshinkai@virus.kyoto-u.ac.jp

Received: 2 April 2008; accepted: 27 August 2008; published online: 25 September 2008

To further elucidate how G9a/GLP-mediated H3K9 methylation is crucial for the regulation of transcriptional silencing and DNA methylation, we established several ES cell lines that express only catalytically inactive mutants of G9a or/and GLP.

Results

Establishment of ES cells expressing G9a-mutant/GLP complexes that cannot catalyse H3K9 methylation in vivo

To elucidate whether G9a/GLP-mediated H3K9 methylation is crucial for transcriptional silencing and DNA methylation of target genes, we wished to establish ES cell lines that express only catalytically inactive mutants of G9a or/and GLP. To establish such ES cell lines, we screened amino-acid substitution or deletion mutants of G9a and GLP SET-domains for their histone methyltransferase (HMTase) activities *in vitro*. On the basis of the crystal structure of another H3K9 HMTase, DIM-5 (Zhang *et al*, 2002), we introduced four different mutations in both G9a and GLP SET-domains (Figure 1A and B). *In vitro* methyltransferase assays using recombinant histone H3/H4 and glutathione *S*-transferase fused to the SET-domains of G9a or GLP showed that each of the G9a and GLP SET-domain mutants were severely impaired for their HMTase activities (<0.1–0.5% catalytic activities of wild-type G9a or GLP SET-domains)(Figure 1C).

We introduced full-length G9a or GLP mutants harbouring one of these mutations (GM3, 4, 6, 7 and LM3, 4, 6, 7) into *G9a*-KO or *GLP*-KO ES cells, respectively (listed in Figure 1D). Whereas the LM3 or LM6 GLP mutants were poorly expressed (~20% of wt GLP level), the remaining mutants were expressed at levels similar to endogenous G9a or GLP (Supplementary Figure S2). As G9a/GLP heteromeric formation is essential for H3K9 methyltransferase activities *in vivo*, we examined the ability of these mutants to form such heteromeric complexes. As shown in Figure 1E and Supplementary Figure S3, G9a and GLP mutants that possess mutation GM3, GM6 or LM3 do not form heteromers. In contrast, the G9a or GLP mutants GM4, GM7, LM4, LM6 or LM7 do form heteromers with their partner molecules. These findings indicate that the NHXC motifs of G9a and GLP SET-domains are essential for both HMTase activity and complex formation, but these two functions are separable.

We next examined the effects of these mutations on H3K9 methyltransferase activity *in vivo* (summarized in Figure 1F). As described previously and shown in Supplementary Figure S4, global H3K9me2 and me1 are dramatically impaired in *G9a*- and *GLP*-KO ES cells and completely restored by stable expression of exogenous wild-type proteins (Tachibana *et al*, 2002, 2005). Among the ES cell lines expressing each G9a or GLP mutant, H3K9 methylation was not recovered in G3, G6 and L3 ES cells, in which mutant G9a or GLP could not form a heteromer (see Figure 1E), confirming that the formation of the G9a/GLP heteromeric complex is essential for their *in vivo* H3K9 methylation. Interestingly, while L4 and L7 ES cells, which express GLP mutants LM4 and LM7, respectively, recovered global H3K9me1 and 2, such methylation was not rescued in G4 and G7 ES cells in which G9a mutants containing GM4 and GM7, respectively, were expressed. As shown in Figure 1E, these G9a and GLP mutants did form heteromeric complexes. Therefore, these data suggest that catalytic activity of GLP but not G9a is dispensable for their H3K9 methyltransferase activities *in vivo*.

Silencing of G9a/GLP-target genes is maintained in ES cells expressing catalytically inactive G9a/GLP complexes

Although it is not clear why catalytic activity of GLP is dispensable for H3K9 methylation *in vivo*, we generated ES cells that express catalytically inactive G9a/GLP heteromeric complexes that do not rescue global H3K9me1 and 2 to elucidate the impact of such mutant complexes on transcriptional silencing. We examined the expression of two of G9a-target genes, *Mage-a* and *Wfdc15a*, shown previously to be targets of G9a and GLP. The *Mage-a* gene, a homologue of one of the cancer-testis antigen genes, is located on the X chromosome (De Plaen *et al*, 1999). The *Wfdc15a* gene is located on mouse chromosome 2 (2 H3). As shown in Figure 2A and B and Supplementary Figure S1, both genes are reactivated in *G9a*- or *GLP*-KO ES cells. Moreover, stable expression of exogenous *WT* genes in the corresponding KO ES cells reestablished transcriptional silencing of these genes (Figure 2A, lanes GW and LW). These observations confirm that transcripts of *Mage-a* and *Wfdc15a* are negatively regulated by the G9a/GLP heteromeric complex. Neither transcript was suppressed in the newly established ES cell lines G3, G6 and L3, indicating again that the formation of G9a/GLP heteromeric complex is necessary for their transcriptional silencing function. However, unexpectedly, G9a/GLP complex-mediated gene suppression was maintained in G4 and G7 ES cells that do not rescue global H3K9me1 and 2 (compare Figures 1F and 2B). To determine whether H3K9 methylation is affected in the promoter region of *Mage-a2* and the 5′-upstream region of *Wfdc15a* in these cells, we carried out chromatin immunoprecipitation (ChIP) analysis in GW, G3, G4, G7, L4 and L7 cells (Figure 2C). Although H3K9 mono- and di-methylation levels at both loci were depleted in the G4 and G7 lines, to a level similar to that observed for the G3 line, these marks were still present in L4 and L7. Profiles of H3K4me2 on the *Mage-a2* promoter in these mutant lines were also examined by ChIP analysis (Figure 2C, top). Among them, only G3 cells showed increased H3K4me2 levels, consistent with the transcriptional activity of the *Mage-a* gene. In contrast, the levels of H3K4me2 on the 5′-upstream region of *Wfdc15a* have less correlation with transcriptional competency compared with those of *Mage-a2* (Figure 2C, bottom). Collectively, these data clearly suggest the existence of a new mechanism of G9a/GLP complex-mediated transcriptional silencing, which occurs independent of H3K9 methylation or HMTase activity. Consistent with our findings, treatment of the G9a-specific inhibitor, BIX-01294, only very poorly reactivated G9a-target genes in murine ES cells (Kubicek *et al*, 2007).

DNA methylation of the G9a/GLP-target promoter regions is maintained in ES cells expressing catalytically inactive G9a/GLP complexes

We next examined the status of CpG methylation on the promoter and 5′-upstream region of G9a/GLP-target genes. We analysed the status of eight CpG sites within the promoter region (0 to −287) and the first CpG site within

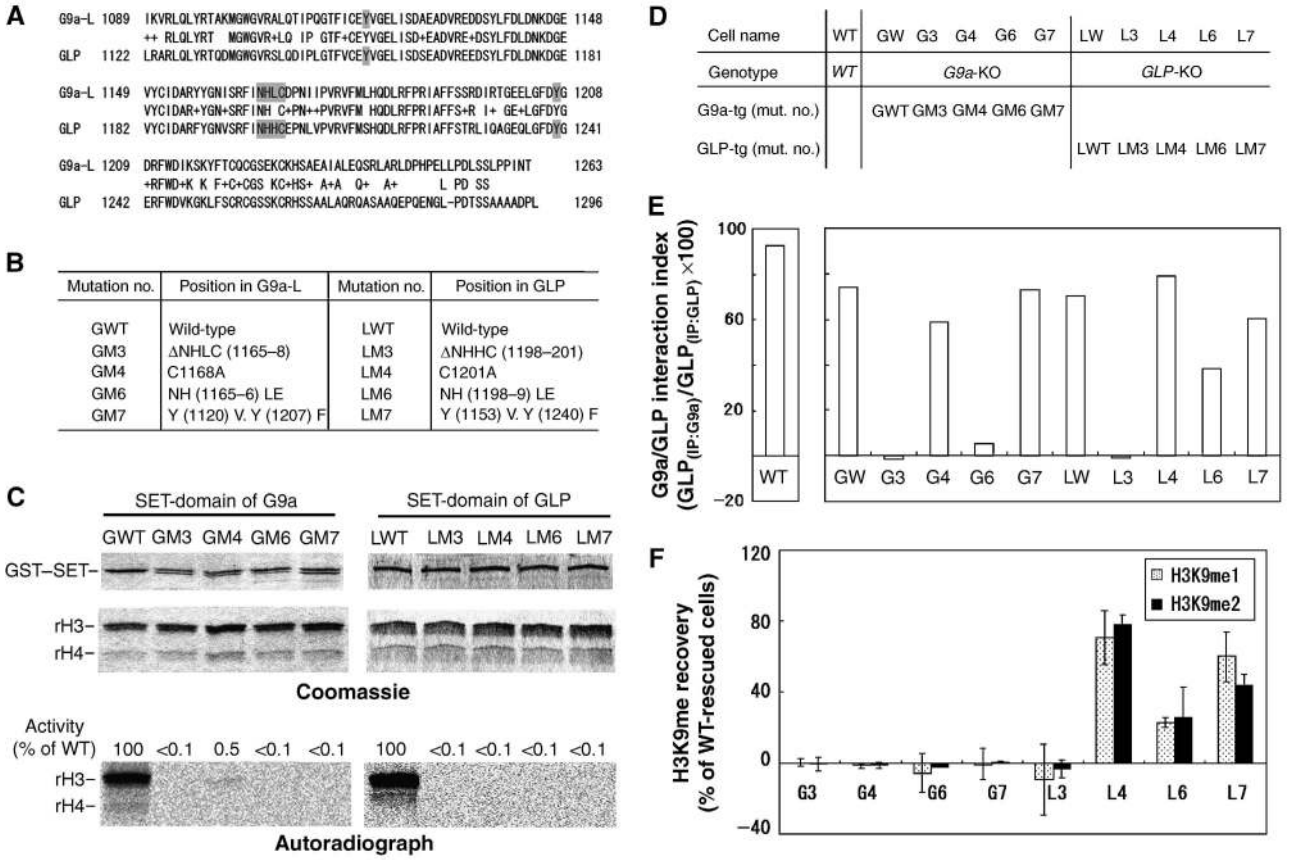

Figure 1 Reconstitution of G9a/GLP complex carrying mutations in their SET-domains. (**A**) Amino-acid alignment of the SET-domains of mG9a-L (Genbank, 21832048) and mGLP (Genbank, 60115440). Conserved and similar residues (shown as +) are shown between the two sequences. Mutagenized amino acids are shown in grey boxes. (**B**) Table showing serial mutants of G9a and GLP. (**C**) *In vitro* histone methyltransferase activity of mutant SET-domains of G9a (left) and GLP (right). GST-fused carboxy terminus of mouse G9a (969-1263 of G9a-L) and that of mouse GLP (1002–1296) were incubated with recombinant histone H3/H4 and *S*-adenosyl-[*methyl*-14C]-L-methionine, and then separated by SDS–PAGE. Coomassie staining shows enzymes and substrates. Autoradiography shows 14C-methyl group incorporated into recombinant H3. Activities of mutant enzymes were quantified using image J (http://rsb.info.nih.gov/ij/) and those of GWT or LWT are normalized to 100%. (**D**) List of ES cell lines expressing mutant G9a/GLP complexes. Serial cell lines were established by stable introduction of the expression plasmids for full-length of G9a-L or GLP into the corresponding KO cells shown in Supplementary Figure S1. Expression levels of mutant G9a or GLP proteins are shown in Supplementary Figure S2. (**E**) The ability of serial mutant proteins to form heterodimers are numerically represented as G9a/GLP interaction index. Protein levels within anti-G9a or anti-GLP immune complexes shown in Supplementary Figure S3 were measured by image J software, and the ratio of GLP protein immunoprecipitated with anti-G9a to those immunoprecipitated with anti-GLP were calculated. The interaction index of wild-type (WT) ES cells (top left panel) is ~100%, indicating that endogenous G9a and GLP form a stoichiometric (1:1) heteromer in wild-type cells. (**F**) H3K9 methylation status of serial mutant ES lines were measured by immunoblot analysis and numerically represented as H3K9me recovery (Raw data are presented in Supplementary Figure S4). The values of signal intensities for methylated H3K9 of GW and LW are normalized to 100%, and those of the corresponding KO cells are normalized to 0%. Data represents an average value of the H3K9 recovery of two clones established independently.

exon one of the *Mage-a2* gene (Figure 3A) and eleven CpG sites in the 5′-upstream of *Wfdc15a* (Figure 3C) by bisulfite sequencing analysis. DNA methylation status of the *Mage-a2* promoter region in the ES lines analysed is summarized in Figure 3B. As described above, all nine CpG sites are heavily methylated in WT cells, whereas those of *G9a*- or *GLP*-KO cells are hypomethylated. Furthermore, those hypomethylation phenotypes can be rescued by introduction of the exogenous corresponding HMTases (see panels *G9a*-KO, *GLP*-KO, GW and LW). Such restoration of DNA methylation was not induced in G3 and L3 cells in which the mutant G9a or GLP does not form a heteromeric complex with endogenous partner. Most importantly, these CpG sites on the *Mage-a2* promoter region were significantly methylated in G4 and G7 cells in which both global and specific H3K9 methylation were not restored, but the G9a/GLP-target genes were nevertheless silent. The pattern of DNA methylation in the 5′-upstream region of *Wfdc15a* was similar to that of the *Mage-a2* promoter region in the ES lines examined—that is, hypermethylated in WT, GW, LW, G4, L4, G7 and L7 cells, but hypomethylated in *G9a*-KO, *GLP*-KO, G3 and L3 ES cells (Figure 3D and E). Protein amounts of Dnmt1, 3a and 3b were not reduced in *G9a*- or *GLP*-KO and several ES cell lines expressing mutant G9a/GLP (Supplementary Figure S2), suggesting that the DNA hypomethylation phenotype was not induced by an intrinsic reduction of DNA methylation machineries. To summarize, these data strongly suggest that the G9a/GLP complex regulates DNA methylation independent of the HMTase activities of these enzymes.

Inhibition of DNA methylation reactivates the G9a/GLP-target genes specifically in the ES cells expressing catalytically inactive G9a/GLP complexes

To further elucidate whether the G9a/GLP complex suppresses target genes through the combination of H3K9 and DNA methylation, we cultured ES cells expressing wt or mutant G9a or GLP in the presence of the DNA methyltransferase inhibitor, 5-Aza-2′-deoxycytidine (5-Aza-dC) or the histone deacetylase inhibitor, tricostatin-A (TSA). As shown in Figure 4A (and summarized in Figure 4C), TSA treatment had no or very small effects on transcriptional activation of *Mage-a* and *Wfdc15a* genes in the examined ES cell lines, including GW, G3, G4, L4, G7 and L7, although global H3 acetylation was drastically increased (Figure 4B). On the other hand, 5′Aza-dC treatment significantly reactivated both genes in G4 and G7 cells (Figure 4A and C) to levels similar to those seen in *G9a*- or *GLP*-KO ES cells without 5′Aza-dC treatment (Figure 2A and data not shown). In contrast, these G9a/GLP-negative target genes were still silent or very mildly reactivated in GW, L4 and L7 cells

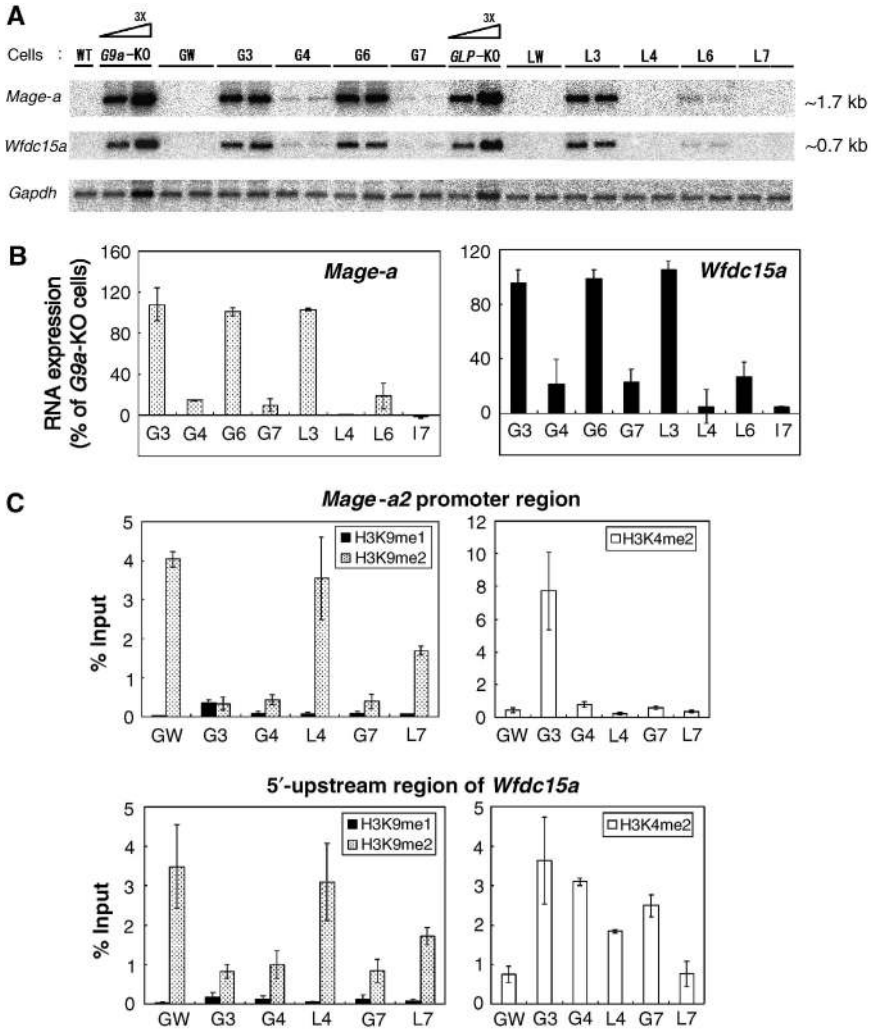

Figure 2 Effect of G9a or GLP mutations on transcriptional suppression. (**A**) Northern blot analyses of *Mage-a* and *Wfdc15a* genes in ES cells expressing mutant G9a/GLP are shown. Total RNA collected from two independent clones were separated and probed with radiolabelled cDNAs. (**B**) Signal intensities for the transcripts of *Mage-a* (left) and *Wfdc15a* (right) were calculated by image J software and numerically represented. The value for *G9a*-KO cells was set at 100%. Data represents an average value between two independent clones. (**C**) Differences in the histone modification patterns on the *Mage-a2* promoter region (top) and 5′-upstream region of *Wfdc15a* (bottom) in the serial ES cell lines were measured by chromatin immunoprecipitation (ChIP) analysis using anti-H3K9me1 and me2 (left) and H3K4me2 (right). Each experiment was performed twice.

Figure 3 G9a/GLP complex formation induces DNA methylation of the *Mage-a2* promoter and the 5′-upstream region of the *Wfdc15a* gene. (**A**) A schematic diagram of CpG positions and amplicon for ChIP analysis within *Mage-a2* promoter is shown. DNA methylation status of eight CpG sequences (no. 1-8) within the promoter (0 to −287) and a CpG (no. 9) located at the 5′ end of the transcribed region were examined in this study. (**B**) Methylation differences among serial ES lines expressing mutant G9a/GLP complex at the *Mage-a2* promoter. DNA methylation status of CpG positions nos. 1–9 shown in (A) was measured by bisulphite sequencing. Open circles indicate unmethylated cytosines and filled circles indicate methylated cytosines. (**C**) Schematic diagram of CpG positions and amplicon for ChIP analysis within the 5′-upstream region of *Wfdc15a*. (**D**, **E**) Methylation differences among serial ES lines expressing mutant G9a/GLP complex at the position no. 1–8 (D) and no. 9–11 (E) of CpG sequences on the 5′-upstream region of *Wfdc15a*.

after the same 5′Aza-dC treatment. We examined the CpG methylation status of G9a-target genes in the 5′Aza-dC-treated cell lines using bisulphite sequencing. As shown in Supplementary Figure S5 (and in comparison with Figure 3B–E), CpG methylation was significantly reduced in all 5′Aza-dC-treated cells, indicating that transcriptional reacti-

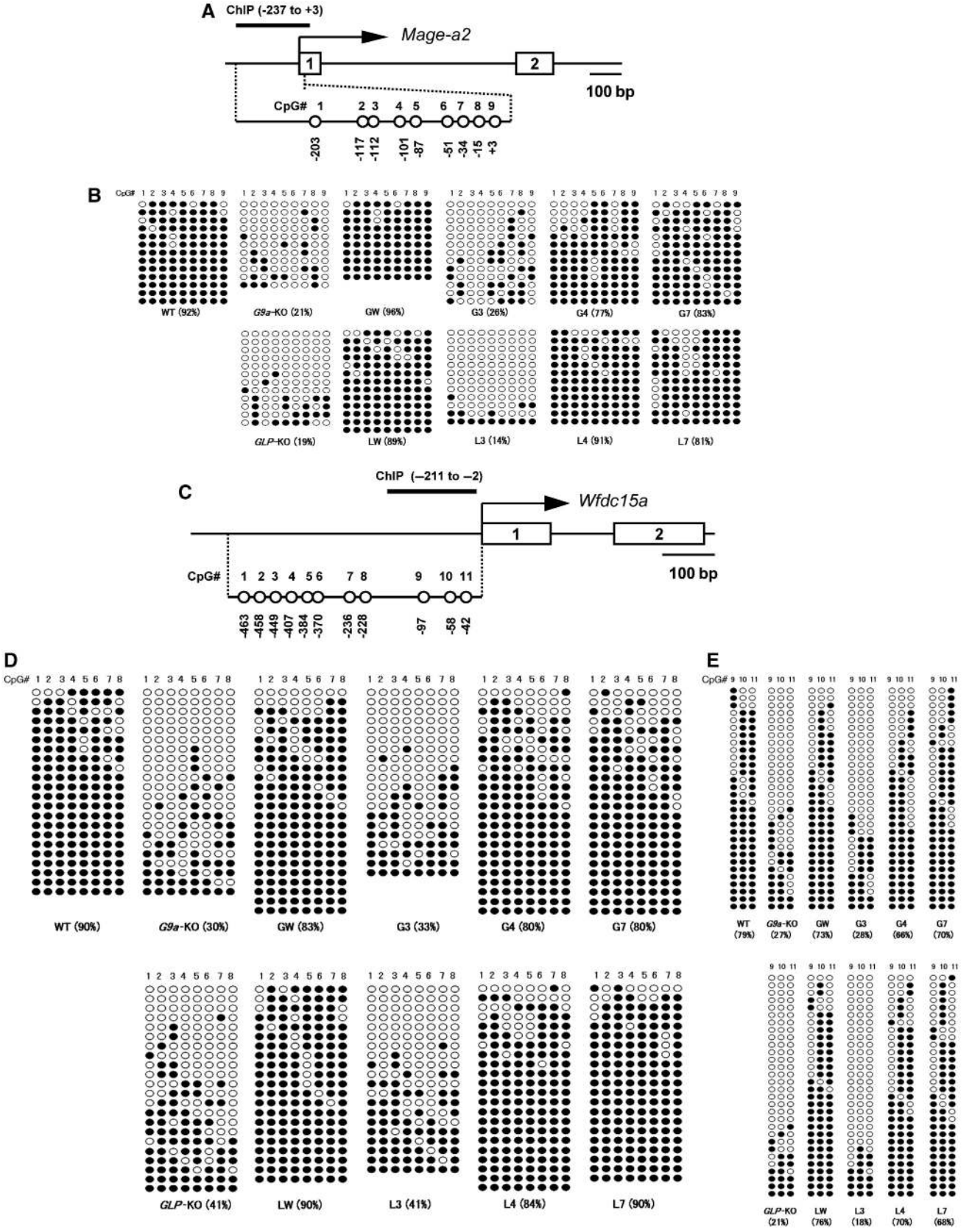

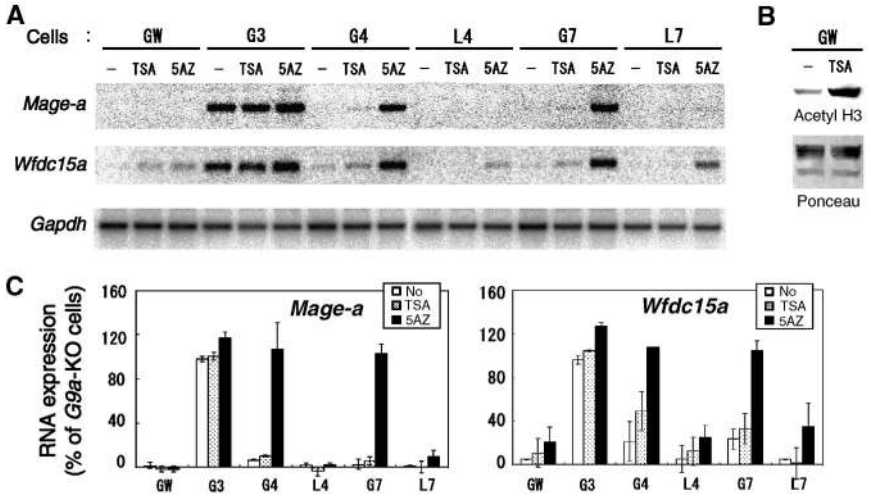

Figure 4 Inhibition of DNA methyltransferase activity reactivates G9a/GLP-target gene expression independent of H3K9 methylation. (**A**) Serial ES lines were cultured with histone deacetylase inhibitor, tricostatin-A (TSA) or the DNA methyltransferase inhibitor, 5-Aza-2′-deoxycytidine (5AZ). Total RNA from treated cells was isolated and analysed through northern blotting using radiolabelled cDNA. (**B**) The effect of TSA on H3 acetylation was confirmed by immunoblot analysis with specific antibodies directed against acetyl histone H3. Ponceau staining represents equal loading of histones. (**C**) Reactivation of the transcripts for *Mage-a* (left) and *Wfdc15a* (right) is represented numerically. The values for *G9a*-KO cells without drug treatment are normalized to 100%. Experiments were performed twice.

vation in G4 and G7 cells was induced by the reduction of DNA methylation. These serial experiments strongly support that the G9a/GLP heteromeric complex induces both H3K9 and DNA methylation on their target gene loci and that these two epigenetic marks cooperatively suppress their targets transcription.

DNA methylation does not direct H3K9 methylation of the G9a/GLP-target genes

Bisulphite sequencing analysis clearly demonstrated that G9a/GLP-regulated DNA methylation is not directed by their HMTase activities or deposited H3K9 methylation, at least on some target gene loci. However, whether DNA methylation or the DNA methylation machinery directs G9a/GLP-mediated transcriptional silencing or H3K9 methylation remains controversial. In humans, *DNA methyltransferase 1 (DNMT1)* knockdown in HeLa cells or *DNMT1*-null HCT116 cells shows a reduction of G9a-mediated H3K9 methylation (Estève *et al*, 2006). On the other hand, no clear reduction of global H3K9 methylation was seen in the *Dnmt1, 3a, 3b* triple mouse KO ES cells (Tsumura *et al*, 2006). To clarify this issue, we analysed the status of transcription of *Mage-a* and *Wfdc15a* genes, DNA methylation and H3K9 methylation of the *Mage-a2* promoter and 5′-upstream of *Wfdc15a* in *Dnmt*-KO ES cells. We utilized *Dnmt1*- and *Dnmt3a+b* double KO (DKO) cells, both of which show a dramatic reduction of DNA methylation (Li *et al*, 1992; Okano *et al*, 1999). As shown in Figure 5A and 5B, *Mage-a* and *Wfdc15a* genes were mostly silent or very poorly transcribed in the *Dnmt*-KO ES cells. However, the CpG sites on the *Mage-a2* promoter region and 5′-upstream of *Wfdc15a* were hypomethylated in both *Dnmt1*-KO and *Dnmt3a+b*-DKO ES cells to levels similar or lower than those of *G9a*- or *GLP*-KO ES cells, respectively (Figure 5C and in comparison with Figure 3B–E). These observations indicate that both Dnmt1 and Dnmt3a+b are involved in DNA methylation on those G9a/GLP-target gene loci. Importantly, the status of H3K9me2 on the *Mage-a2* promoter region and 5′-upstream region of *Wfdc15a* were maintained in both *Dnmt1*-KO and *Dnmt3a+b*-DKO ES cells at levels similar to those of wild-type ES cells (Figure 5D). These facts clearly suggest that G9a/GLP-mediated H3K9 methylation at G9a/GLP-target gene loci are not directed by the DNA methyltransferase machinery or deposited DNA methylation. Furthermore, the phenotypes of *Dnmts*-KO ES cells indicate that G9a/GLP-mediated H3K9 methylation can suppress transcription even in the absence of DNA methylation. To identify the *de novo* DNA methylation enzyme(s) responsible for the regulation of G9a/GLP-target gene loci, we analysed CpG methylation status in several *Dnmt3a+b* DKO ES lines that stably expressed exogenous *Dnmt3a1, 3a2* or *3b1* ((Oda *et al*, 2006), Figure 6A and B). Methylation of the CpG sites on *Mage-a2* and *Wfdc15a* was significantly recovered in all the rescued *Dnmt3a+b* DKO ES cell lines expressing Dnmt3a1, 3a2 or 3b1 (in comparison of Figure 6B with 5C). The relatively poor expression of exogenous Dnmt3b1 may account for the 'partially rescued' phenotype (Figure 6A). Collectively, these genetic data suggest that both Dnmt3a and 3b redundantly regulate DNA methylation at G9a/GLP-target loci.

Discussion

In this report, we demonstrate that the G9a/GLP heteromeric complex regulates both H3K9 and DNA methylation and that these two epigenetic marks cooperatively silence transcription. However, these two epigenetic marks are deposited independent of one another (see model—Figure 7).

How does the G9a/GLP complex regulate DNA methylation at the molecular level? G9a/GLP-target genes were fully reactivated in G4 or G7 cells in the presence of 5′Aza-dC, suggesting that induction of DNA methylation on those G9a/GLP-target genes is directed by the G9a/GLP complex rather

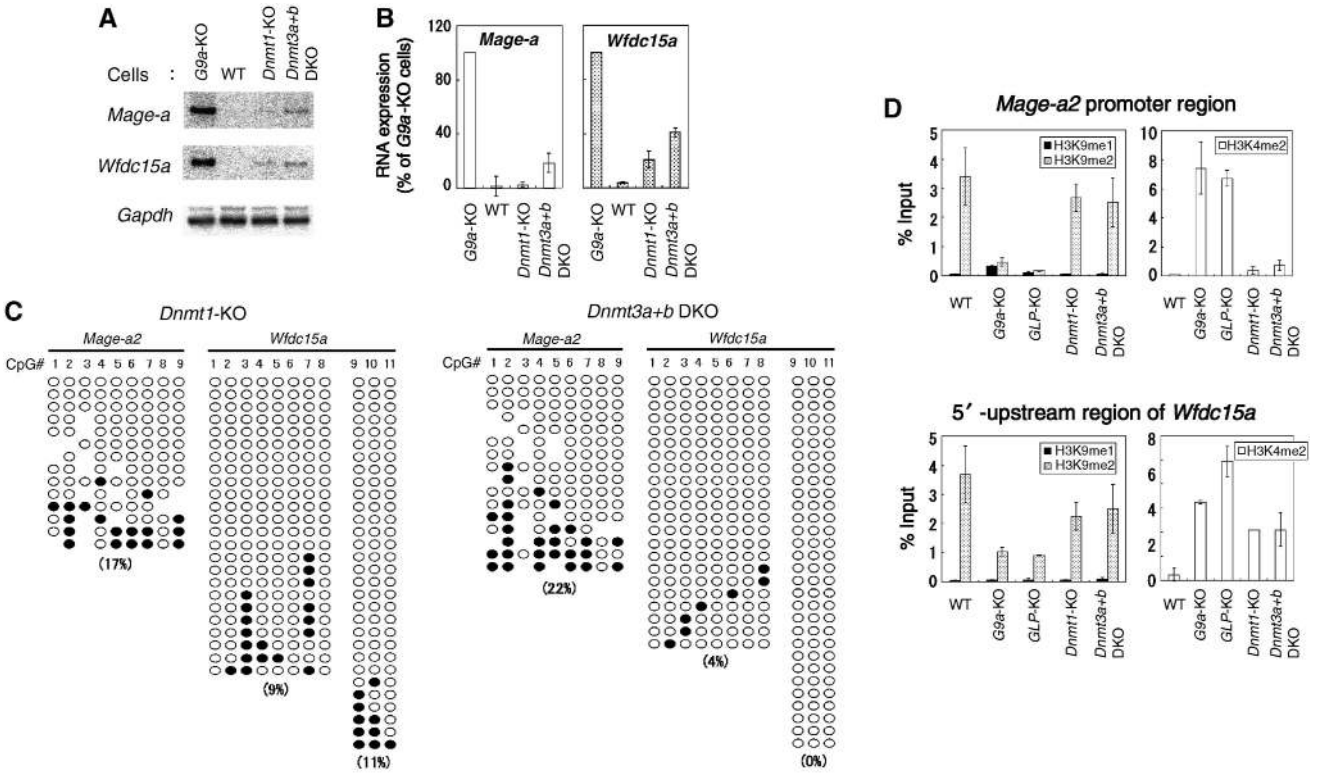

Figure 5 H3K9 methylation suppresses G9a/GLP-target genes in DNA methyltransferase-deficient ES cells. (**A**) Northern blot analyses of *Dnmts*-KO ES cells are shown. Total RNA was separated and probed with radiolabelled cDNAs. (**B**) Expression levels for *Mage-a* (left) and *Wfdc15a* (right) are numerically represented. The values for *G9a*-KO cells are normalized to 100%. Each experiment was carried out twice. (**C**) Cytosine methylation status of *Mage-a2* promoter and 5′-upstream region of *Wfdc15a* in *Dnmt1*-KO (left) and *Dnmt3a* + *b* DKO (right) ES cells. CpG positions are as described in Figure 3B and D. (**D**) Histone methylation patterns of the *Mage-a2* promoter region (top) and 5′-upstream region of *Wfdc15a* (bottom) in *Dnmts*-KO ES cells were determined by ChIP analyses. H3K9me2 around the promoter is still maintained in *Dnmt1*-KO and *Dnmt3a* + *b* DKO ES cells. Experiments were carried out twice.

than a lack of transcriptional competence. One simple mechanism is that the G9a/GLP heteromeric complex directly recruits the DNA methyltransferase(s)/DNA methyltransferase machinery. Indeed, it has been reported that human G9a interacts with DNMT1 (Estève *et al*, 2006) and HP1 interacts with DNMT1 (Smallwood *et al*, 2007). Furthermore, our proteomics analysis shows that HP1 (mainly HP1γ) is in the G9a/GLP complex in mouse ES cells (data not shown). However, we have been unable to detect an association between G9a(/GLP) and Dnmt1 in ES cells (data not shown). The DNA methylation phenotypes of *Mage-a2* and *Wfdc15a* also suggest that the G9a/GLP complex induces *de novo* DNA methylation. Therefore, G9a/GLP may associate with *de novo* DNA methyltransferases. Although genetic evidence indicates that the *de novo* DNA methyltransferases Dnmt3a and 3b are responsible for DNA methylation at the G9a/GLP-target loci (Figure 6B), our anti-G9a/GLP or anti-Dnmt3s co-IP experiments fail to detect clear G9a/GLP-Dnmt3 s association in ES cells (data not shown). We have also performed ChIP analysis using antibodies against G9a, GLP and Dnmts and confirmed immunoprecipitation of those molecules from the formalin-fixed samples, but so far we are unable to obtain reliable data exhibiting enrichment of G9a/GLP and Dnmts at specific loci including *Mage-a2* and *Wfdc15a* or showing a good correlation between the DNA methylation phenotypes and enrichment of specific Dnmts (data not shown). Targeting of G9a/GLP or Dnmts may be quite transient or enrichment of ChIPed G9a/GLP- or Dnmts-nucleosomes may be too low to show significant data.

How is the G9a/GLP-mediated DNA methylation phenotype relevant to global DNA methylation? Although we do not detect as dramatic reduction of CpG methylation in *G9a*-KO ES cells as shown in *Dnmt1*- or *Dnmt3a* + *b*-DKO ES cells (not shown), Dong *et al.* describe that *G9a*-KO ES cells show a drastic reduction in DNA methylation of endogenous retroelements, which represent 5–10% of the mammalian genome (Dong *et al*, 2008). They also show that G9a-mediated DNA methylation of the retroelements is independent of its catalytic activity, which is consistent with our findings. If G9a/GLP is required only for *de novo* DNA methylation, depletion of DNA methylation in the *G9a*-KO or *GLP*-KO lines may be minimized by maintenance of methyltransferase activity. To clarify how this G9a/GLP-mediated DNA methylation system is maintained or effective in different types of cells, we examined CpG methylation status of the G9a-target loci in *G9a*-KO embryos (E9.5). Interestingly, but in contrast to *G9a*- or *GLP*-KO ES cells, *G9a*-KO embryos (E9.5) did not exhibit a DNA hypomethylation phenotype at G9a-target gene loci (Supplementary Figure S6). As global H3K9 methylation is severely affected in E9.5 *G9a*-KO embryos in the same way as in *G9a*-KO ES cells (Tachibana *et al*, 2002), these data suggest that the G9a/GLP-independent regulation mechanism(s) also controls CpG methylation of the G9a-taget loci in cells of E9.5 embryos.

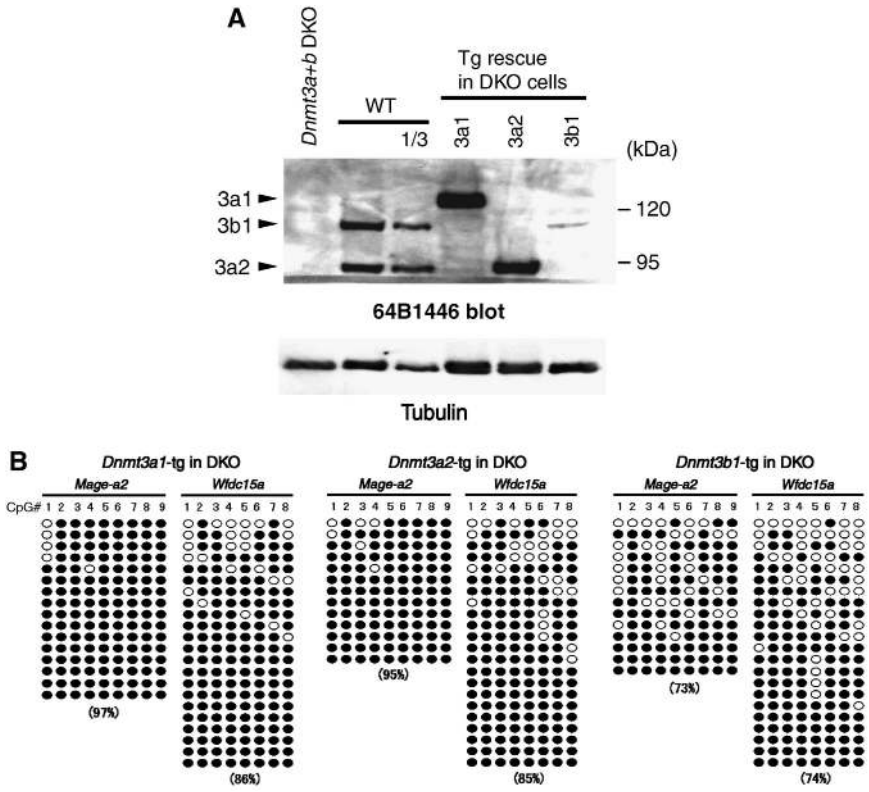

Figure 6 Dnmt3a and 3b redundantly methylate CpG sequences on G9a/GLP-target genes. (**A**) Dnmt3 protein expression of several rescued ES lines on *Dnmt3a + b* DKO background, were analysed with mouse monoclonal antibody 64B1446, which recognizes carboxy terminus of both Dnmt3a and 3b (Chen *et al*, 2002). (**B**) Cytosine methylation status of *Mage-a2* promoter and 5′-upstream region of *Wfdc15a* in Dnmt3-rescued line. CpG positions are as described in Figure 3B and D.

What is the biological significance of the dual silencing mechanism of G9a/GLP seen in ES cells? Compared with differentiated somatic cells, pluripotent ES cells maintain a chromatin structure that is generally permissive for transcriptional activation including relatively low overall levels of DNA methylation (Kimura *et al*, 2004; Meshorer and Misteli, 2006). In this regard, ES cells may effectively utilize the dual methylation system observed here to secure the silencing state of G9a/GLP-target gene loci upon cellular differentiation. Another possible benefit is that such dual silencing mechanism can also stably maintain the silent status throughout differentiation of specific lineage of cells. DNA methylation is quite dynamically regulated during development of specific lineage of cells, such as germ-lineage cells (Reik *et al*, 2001; Surani, 2001). During temporal loss of DNA methylation in certain developmental stages, the silent states can be maintained if the G9a/GLP dual silencing mechanism regulates gene transcription (similar to the case of *Dnmts*-KO in Figure 7). This mechanism also applies to the dynamics of H3K9 methylation regulated by HMTases and histone lysine demethylases or other mechanisms (Klose and Zhang, 2007; Shi, 2007). Lastly, our data suggest that other epigenetic marks also function as one of multiple layers of regulatory mechanisms.

Materials and methods

In vitro HMTase assay

Methyltransferase assays were performed as described previously (Tachibana *et al*, 2001). Briefly, 15 μl of reaction mixture containing 1 μg of recombinant H3/H4, 1 μg of recombinant enzymes and 50 nCi of *S*-adenosyl-[*methyl*-14C]-L-methionine in methylase activity buffer (50 mM Tris, pH 8.5, 20 mM KCl, 10 mM $MgCl_2$, 10 mM β-mercaptoethanol, 250 mM sucrose) was incubated for 120 min at room temperature. The reaction products were separated by 15% SDS–PAGE. Detection of *methyl*-14C was performed using a BAS-5000 imaging analyser (Fuji Film).

Cell culture

Embryonic stem cells were maintained in Dulbecco's modified Eagle's medium (Sigma) containing 10% Knockout SR (Invitrogen) and 1% fetal calf serum (described as ES medium hereafter). To generate ES cells stably expressing mutant G9a or GLP, the expression vectors designated as pCAG-G9a-L-IRESpuro or pCAG-GLP-IRESbsd were introduced into the corresponding KO ES cells by using Lipofectamine 2000 reagent (Invitrogen). The stable transfectant clones expressing mutant G9a or GLP were selected in the ES medium containing puromycin (1 μg/ml) or blasticidin (10 μg/ml), respectively. For northern blot analysis, ES cells were cultured in the ES medium with tricostatin-A (10 ng/ml) for 24 h or 0.5 μM 5-Aza-2′-Deoxycytidine for 96 h.

G9a/GLP complex formation analysis

Serial ES lines were harvested with PBS containing 0.05% trypsin and 0.2 mM EDTA. The cellular pellets were washed once in ice-cold PBS, snap-frozen in liquid nitrogen and stored at −80 °C before analysis. For G9a/GLP interaction analysis, the cellular pellets were lysed with RIPA buffer (PBS containing 1% NP40, 0.5% deoxycholate, 0.1% SDS and protease inhibitor cocktail (Nakalai)). The cellular extracts were prepared by removing unresolved pellets after centrifugation, and then incubated with 2 μg of either anti-G9a (A8620A, Perseus Proteomix) or anti-GLP (B0422, Perseus Proteomix) overnight. The immune complexes were collected with 15 μl of protein G slurry (1:1 ratio, GE Healthcare) for 3 h, washed three times with PBS containing 0.1% NP40 and then separated by SDS–PAGE.

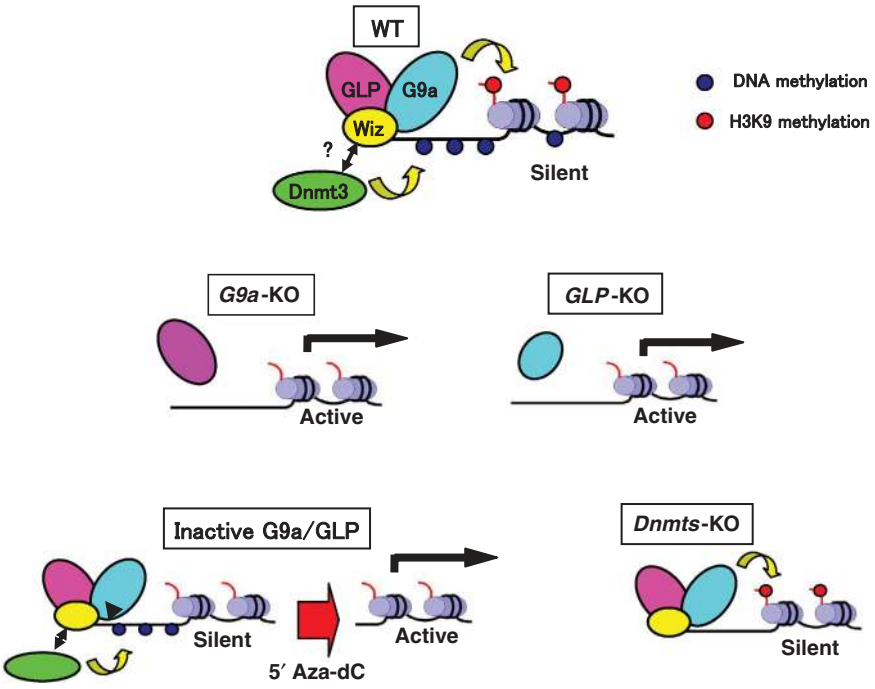

Figure 7 Schematic representation of G9a/GLP complex-mediated gene suppression. One candidate molecule links G9a/GLP to DNA methyltransferase is Wiz, as it binds preferentially G9a/GLP heteromer (Ueda *et al*, 2006). Genetic analyses indicate that orphan G9a (right) or GLP (left) is both incapable of catalysing H3K9 methylation and recruiting DNA methylation, accompanied with the reactivation of the target genes (see panels of *G9a*-KO and *GLP*-KO). Mutant complex incapable of H3K9 methylation, such as GM4/LWT or GM7/LWT, can still suppress transcription via recruiting DNA methyltransferase(s) (see panels of inactive G9a/GLP). This suppression is cancelled by 5′Aza-dC treatment. G9a/GLP complex can also suppress transcription even without DNA methylation, solely by depositing H3K9 methylation (see panel of *Dnmts*-KO).

Histone modification analysis

Histones corresponding to 5×10^4 nuclei were purified by acid extraction (Tachibana *et al*, 2002), separated by SDS–PAGE, transferred to nitrocellulose membranes, blocked with 5% milk and probed with the specific antibodies against H4 (Millipore, 07-108), H3K9me1 (Millipore, 07-450), H3K9me2 (Millipore, 07-441) and H3K9me3 (Millipore, 07-523).

For ChIP analysis, we slightly modified the previous protocols for native ChIP analysis (O'Neill and Turner, 1995; Gregory *et al*, 2001). ES cells ($\sim 5 \times 10^6$) suspended in 50 μl of 0.3 M sucrose-containing buffer 1 (60 mM KCl, 15 mM NaCl, 5 mM $MgCl_2$, 0.1 mM EGTA, 0.5 mM dithiothreitol, 0.1 mM PMSF, 3.6 ng/ml aprotinin, 15 mM Tris–HCl pH 7.5) were lysed by addition of 50 μl of buffer 1 containing 0.8% NP40 and 0.3 M sucrose and put on ice for 10 min. After addition of 0.8 ml of buffer 1 containing 1.2 M sucrose to the suspension, chromatin fraction was collected as pellets by centrifugation (8500 r.p.m., 10 min). The pellets were resuspended in 200 μl of micrococcal nuclease (MNase) digestion buffer (0.32 M sucrose, 4 mM $MgCl_2$, 1 mM $CaCl_2$, 0.1 mM PMSF, 50 mM Tris–HCl pH 7.5), incubated at 37 °C for 15 min with MNase (0.3–0.6 U, Takara). Digestion was stopped by addition of EDTA to a final concentration of 20 mM. Approximately 200 μl of the supernatant was obtained by centrifugation (13000 r.p.m., 10 min), combined with 1.8 ml of incubation buffer (50 mM NaCl, 5 mM EDTA, 0.1% NP40, 0.1 mM PMSF, 20 mM Tris–HCl pH 7.5), incubated overnight with antibodies against methylated H3 and then incubated for further 4 h after addition of 15 μl of protein G slurry (1:1 ratio, GE Healthcare). Antibodies used were mouse monoclonal antibodies against H3K9me1 (CMA306), H3K9me2 (ab1220, Abcam) and H3K4me2 (CMA303) (Kimura *et al*, 2008). The immune complexes were sequentially washed in 75 mM NaCl-containing buffer A (75 mM NaCl, 10 mM EDTA, 50 mM Tris–HCl pH 7.5), 125 mM NaCl-containing buffer A and 175 mM NaCl-containing buffer A. DNA was obtained by phenol/chloroform extraction following proteinase K treatment (0.1 mg/ml) of the immune complex in digestion buffer (400 mM NaCl, 10 mM EDTA, 0.5% SDS, 20 mM Tris–HCl pH 8.0, 0.1 mg/ml proteinase K) for 60 min at 56 °C, and then analysed by real-time PCR using primers specific for *Mage-a2* promoter (Mage-a2A, 5′-TTGGTGGACAGGGAAGCTAGGGGA-3′; Mage-a2B, 5′-CGCTCCAGAACAAAATGGCGCAGA-3′), and 5′-upstream region of *Wfdc15a* (AV2P.4, 5′-GGATAACCAGCAGGGAAGCTGAGG-3′; AV2P.5, 5′-TCTCTAGGTGCCTGAACCTACAGC-3′).

DNA methylation analysis

Bisulphite treatment of the genomic DNA isolated from serial ES lines was carried out with EpiTect bisulfite Kit (Qiagen). Nested PCR was performed to amplify the sequences around the *Mage-a2* promoter and 5′-upstream region of *Wfdc15a*. The first-round PCR (35 cycles) and the second-round PCR (20 cycles) were carried out using specific primer sets as follows. For CpG position no. 1–9 of *Mage-a2* (see Figure 3A), Magea2.1bi (5′-GGATTTTGAAAGA AATGGTGATTT-3′) and Magea2.2bi (5′-AATTCTTACCTCAACTAAC ACAAC- 3′) were used for the first-round PCR and Magea2-NesF-bi-Bam (5′-ATAGGATCCTATATTGGTGGATAGGGAAGTTAGGG-3′) and Magea2-R-bi-RI (5′-ATAGAATTCTCAACTAACACAACATAAAAACCT CC-3′) were used for the second-round PCR. For CpG position no. 1–8 of *Wfdc15a* (see Figure 3C), SAV-bi.b (5′-TTGGTGTTTAGGTAG ATATAGTTAATAAGA-3′) and SAV2bi.d (5′-CTTCTTAAAAACTAACA AAACTAATCTAACATTTC-3′) were used for the first-round PCR and SAV-nes-BF-2 (5′-ATAGGATCCAAGGAAAATGTATTTATAAATTAA AG-3′) and SAV-nes-RR-3 (5′-TATGAATTCAAAACTAATCTAACATTT CCTAATAC-3′) were used for the second-round PCR. For CpG position no. 9–11 of *Wfdc15a*, AV2bi.1 (5′-GGATAATTAGTAGGGA AGTTGAGG-3′) and AV2bi.4 (5′-ACCAAACTAACCCTACTAATCCC TA-3′) were used for the first-round PCR and AVbi.1-RI (5′-ATAGAAT TCAAGTTGAGGTTATAGGTTAGG-3′) and AV2bi.4-Bam (5′-TAAG GATCCAAAACATTATCTTCCTTCCTC-3′) were used for the second-round PCR. The second-round PCR products were subcloned into pBluescript vectors digested with *Eco*RI and *Bam*HI.

RNA expression analysis

Total RNAs were isolated with Sepasol-RNA I (Nakarai). Three micrograms of them were separated by 1% agarose-formaldehyde gel electrophoresis, transferred to a nylon membrane, and probed with ^{32}P-labelled cDNAs as follows. The subcloned RT–PCR products corresponding to nucleotides 321–780 of GenBank entry NM_020020 (*Mage-a8*), 28–475 of AV206552 (*Wfdc15a*) and 247-1120 of BC083080 (*Gapdh*) were used as probes.

Supplementary data
Supplementary data are available at *The EMBO Journal* Online (http://www.embojournal.org).

Acknowledgements

We are grateful to Dr E Li (Novartis) and Dr M Okano (RIKEN) for providing *Dnmts*-KO ES cells, the rescued ES lines and specific antibody against Dnmts, and Drs R Hirasawa and H Sasaki (NIG) for technical advices. We thank Dr M Lorincz (The University of British Columbia) for valuable scientific comments and editorial help and our laboratory members for assistance. We also thank Dr EM Oltz for critically reading the manuscript. This work was supported by a Grant-in-Aid from the Ministry of Education, Science, Technology and Culture of Japan.

References

Bannister A, Zegerman P, Partridge J, Miska E, Thomas J, Allshire R, Kouzarides T (2001) Selective recognition of methylated lysine 9 on histone H3 by the HP1 chromo domain. *Nature* **410:** 120–124

Bird A (2002) DNA methylation patterns and epigenetic memory. *Genes Dev* **16:** 6–21

Bostick M, Kim J, Estève P, Clark A, Pradhan S, Jacobsen S (2007) UHRF1 plays a role in maintaining DNA methylation in mammalian cells. *Science* **317:** 1760–1764

Chen T, Ueda Y, Xie S, Li E (2002) A novel Dnmt3a isoform produced from an alternative promoter localizes to euchromatin and its expression correlates with active *de novo* methylation. *J Biol Chem* **277:** 38746–38754

De Plaen E, De Backer O, Arnaud D, Bonjean B, Chomez P, Martelange V, Avner P, Baldacci P, Babinet C, Hwang S, Knowles B, Boon T (1999) A new family of mouse genes homologous to the human MAGE genes. *Genomics* **55:** 176–184

Dong KB, Maksakova IA, Mohn F, Leung D, Appanah R, Lee S, Yang HW, Lam LL, Mager DL, Schübeler D, Tachibana M, Shinkai Y, Lorincz MC (2008) DNA methylation in ES cells requires the lysine methyltransferase G9a but not its catalytic activity. *EMBO J*; E-pub ahead of print 25 September 2008

Estève P, Chin H, Smallwood A, Feehery G, Gangisetty O, Karpf A, Carey M, Pradhan S (2006) Direct interaction between DNMT1 and G9a coordinates DNA and histone methylation during replication. *Genes Dev* **20:** 3089–3103

Feldman N, Gerson A, Fang J, Li E, Zhang Y, Shinkai Y, Cedar H, Bergman Y (2006) G9a-mediated irreversible epigenetic inactivation of Oct-3/4 during early embryogenesis. *Nat Cell Biol* **8:** 188–194

Gregory R, Randall T, Johnson C, Khosla S, Hatada I, O'Neill L, Turner B, Feil R (2001) DNA methylation is linked to deacetylation of histone H3, but not H4, on the imprinted genes Snrpn and U2af1-rs1. *Mol Cell Biol* **21:** 5426–5436

Ikegami K, Iwatani M, Suzuki M, Tachibana M, Shinkai Y, Tanaka S, Greally J, Yagi S, Hattori N, Shiota K (2007) Genome-wide and locus-specific DNA hypomethylation in G9a deficient mouse embryonic stem cells. *Genes Cells* **12:** 1–11

Jackson J, Lindroth A, Cao X, Jacobsen S (2002) Control of CpNpG DNA methylation by the KRYPTONITE histone H3 methyltransferase. *Nature* **416:** 556–560

Jenuwein T (2006) The epigenetic magic of histone lysine methylation. *FEBS J* **273:** 3121–3135

Kimura H, Hayashi-Takanaka Y, Goto Y, Takizawa N, Nozaki N (2008) Organization of histone H3 modifications revealed by a panel of specific monoclonal antibodies. *Cell Struct Funct* **33:** 61–73

Kimura H, Tada M, Nakatsuji N, Tada T (2004) Histone code modifications on pluripotential nuclei of reprogrammed somatic cells. *Mol Cell Biol* **24:** 5710–5720

Klose R, Zhang Y (2007) Regulation of histone methylation by demethylimination and demethylation. *Nat Rev Mol Cell Biol* **8:** 307–318

Kubicek S, O'Sullivan R, August E, Hickey E, Zhang Q, Teodoro M, Rea S, Mechtler K, Kowalski J, Homon C, Kelly T, Jenuwein T (2007) Reversal of H3K9me2 by a small-molecule inhibitor for the G9a histone methyltransferase. *Mol Cell* **25:** 473–481

Lachner M, O'Carroll D, Rea S, Mechtler K, Jenuwein T (2001) Methylation of histone H3 lysine 9 creates a binding site for HP1 proteins. *Nature* **410:** 116–120

Li E, Bestor T, Jaenisch R (1992) Targeted mutation of the DNA methyltransferase gene results in embryonic lethality. *Cell* **69:** 915–926

Margueron R, Trojer P, Reinberg D (2005) The key to development: interpreting the histone code? *Curr Opin Genet Dev* **15:** 163–176

Meshorer E, Misteli T (2006) Chromatin in pluripotent embryonic stem cells and differentiation. *Nat Rev Mol Cell Biol* **7:** 540–546

O'Neill L, Turner B (1995) Histone H4 acetylation distinguishes coding regions of the human genome from heterochromatin in a differentiation-dependent but transcription-independent manner. *EMBO J* **14:** 3946–3957

Oda M, Yamagiwa A, Yamamoto S, Nakayama T, Tsumura A, Sasaki H, Nakao K, Li E, Okano M (2006) DNA methylation regulates long-range gene silencing of an X-linked homeobox gene cluster in a lineage-specific manner. *Genes Dev* **20:** 3382–3394

Okano M, Bell D, Haber D, Li E (1999) DNA methyltransferases Dnmt3a and Dnmt3b are essential for *de novo* methylation and mammalian development. *Cell* **99:** 247–257

Reik W, Dean W, Walter J (2001) Epigenetic reprogramming in mammalian development. *Science* **293:** 1089–1093

Sharif J, Muto M, Takebayashi S, Suetake I, Iwamatsu A, Endo T, Shinga J, Mizutani-Koseki Y, Toyoda T, Okamura K, Tajima S, Mitsuya K, Okano M, Koseki H (2007) The SRA protein Np95 mediates epigenetic inheritance by recruiting Dnmt1 to methylated DNA. *Nature* **450:** 908–912

Shi Y (2007) Histone lysine demethylases: emerging roles in development, physiology and disease. *Nat Rev Genet* **8:** 829–833

Smallwood A, Estève P, Pradhan S, Carey M (2007) Functional cooperation between HP1 and DNMT1 mediates gene silencing. *Genes Dev* **21:** 1169–1178

Strahl B, Allis C (2000) The language of covalent histone modifications. *Nature* **403:** 41–45

Surani M (2001) Reprogramming of genome function through epigenetic inheritance. *Nature* **414:** 122–128

Tachibana M, Sugimoto K, Fukushima T, Shinkai Y (2001) Set domain-containing protein, G9a, is a novel lysine-preferring mammalian histone methyltransferase with hyperactivity and specific selectivity to lysines 9 and 27 of histone H3. *J Biol Chem* **276:** 25309–25317

Tachibana M, Sugimoto K, Nozaki M, Ueda J, Ohta T, Ohki M, Fukuda M, Takeda N, Niida H, Kato H, Shinkai Y (2002) G9a histone methyltransferase plays a dominant role in euchromatic histone H3 lysine 9 methylation and is essential for early embryogenesis. *Genes Dev* **16:** 1779–1791

Tachibana M, Ueda J, Fukuda M, Takeda N, Ohta T, Iwanari H, Sakihama T, Kodama T, Hamakubo T, Shinkai Y (2005) Histone methyltransferases G9a and GLP form heteromeric complexes and are both crucial for methylation of euchromatin at H3-K9. *Genes Dev* **19:** 815–826

Tamaru H, Selker E (2001) A histone H3 methyltransferase controls DNA methylation in *Neurospora crassa*. *Nature* **414:** 277–283

Tsumura A, Hayakawa T, Kumaki Y, Takebayashi S, Sakaue M, Matsuoka C, Shimotohno K, Ishikawa F, Li E, Ueda H, Nakayama J, Okano M (2006) Maintenance of self-renewal ability of mouse embryonic stem cells in the absence of DNA methyltransferases Dnmt1, Dnmt3a and Dnmt3b. *Genes Cells* **11:** 805–814

Ueda J, Tachibana M, Ikura T, Shinkai Y (2006) Zinc finger protein Wiz links G9a/GLP histone methyltransferases to the co-repressor molecule CtBP. *J Biol Chem* **281:** 20120–20128

Wade P (2001) Methyl CpG-binding proteins and transcriptional repression. *Bioessays* **23:** 1131–1137

Xin Z, Tachibana M, Guggiari M, Heard E, Shinkai Y, Wagstaff J (2003) Role of histone methyltransferase G9a in CpG methylation of the Prader–Willi syndrome imprinting center. *J Biol Chem* **278:** 14996–15000

Zhang X, Tamaru H, Khan S, Horton J, Keefe L, Selker E, Cheng X (2002) Structure of the *Neurospora* SET domain protein DIM-5, a histone H3 lysine methyltransferase. *Cell* **111:** 117–127

